



Cite this: *Environ. Sci.: Nano*, 2026, 13, 2341

## Size-dependent UVB-mediated and mechanical breakdown of polystyrene nanoparticles in the presence of iron oxide

Mikael T. Ekvall,<sup>ab</sup> Raluca Svensson,<sup>ab</sup> Swathi Sudhakar,<sup>id</sup> c Ethayaraja Mani,<sup>id</sup> d  
Martin Lundqvist<sup>id</sup> ab and Tommy Cedervall<sup>id</sup> \*ab

Nanoplastics are increasingly being recognized as a global pollutant. However, relatively few studies report directly measured concentrations of nano- and microplastics in environmental samples, although available data suggest levels of up to 0.5 mg L<sup>-1</sup> in lake water, which is surprisingly high. Their degradation in the environment, particularly under UV irradiation, is still poorly understood. Here, we investigated the effect of UVB irradiation on polystyrene nanoparticles of different sizes (99 nm to 200 nm) and evaluated whether iron oxide nanoparticles accelerate their breakdown. Particle size and mass changes were monitored using differential centrifugal sedimentation (DCS), dynamic light scattering (DLS), and nanoparticle tracking analysis (NTA). Our results show that UV-mediated degradation was size-dependent, with larger nanoparticles breaking down more rapidly than the smaller ones under identical mass concentrations. The addition of iron oxide nanoparticles accelerated the UVB-mediated breakdown of the 99 nm particles, leading to a >100-fold reduction in particle concentration and loss of toxicity in *Daphnia magna* assays after 111 days. Mechanical breakdown experiments demonstrated that the larger particles were more susceptible to size reduction than the smaller particles. Together, these findings suggested that small nanoplastic particles may accumulate in natural environments due to their slower degradation, but iron oxide could serve as an effective and low-cost remediation strategy for accelerating their breakdown and mitigating toxicity.

Received 16th September 2025,  
Accepted 18th March 2026

DOI: 10.1039/d5en00848d

rs.li/es-nano

### Environmental significance

Nanoplastics represent a significant and universal environmental pollutant, with their presence reported in remote ecosystems and urban waterways. Given the disturbing concentrations reported, understanding their degradation mechanisms is critical. This study investigates the degradation of polystyrene nanoparticles under UVB irradiation, revealing that the larger nanoparticles degrade more quickly than the smaller ones. The introduction of iron oxide nanoparticles accelerates the breakdown of the 99 nm polystyrene particles. These findings underscore the potential of using iron oxide as a remediation strategy for nanoplastics, emphasizing the need for effective management approaches to mitigate the accumulation and ecological impact of nanoplastics in natural environments.

### Introduction

Nanoplastics have been detected worldwide, even in places that are far from dense human settlements. These places include the North Sea,<sup>1</sup> Atlantic,<sup>2</sup> Austrian Alps,<sup>3</sup> North and South poles,<sup>4</sup> Siberian lakes,<sup>5</sup> and water near urban areas.<sup>5,6</sup> Measuring nanoplastic concentrations is still challenging; however, available data range from low concentrations in the Austrian Alps (46 ng mL<sup>-1</sup> in melted surface snow<sup>3</sup>) to surprisingly high concentrations (563 ng mL<sup>-1</sup>) in waterways near urban areas.<sup>5</sup> Studies comparing the amount of nano- and

micro-plastics in the same area or organism are rare. However, the mass of nanoplastics in the Atlantic was reported to be equal to or greater than the combined mass of micro- and macro-plastics.<sup>2</sup> In mussels, the amount of nanoplastics in the size range of 20–200 nm was 187 ng mg<sup>-1</sup> dry weight, which is close to the amount of nanoplastics of sizes above 2.2 μm (218 ng mg<sup>-1</sup> dry weight).<sup>7</sup> Interestingly, in a recent study on microplastics deposited in the human lungs, 97% of the particles (in number) were between 1 and 10 μm and only 3% were of sizes larger than 10 μm.<sup>8</sup> However, the detection of smaller particles was not included in this study. Acknowledging that there is a need for more studies, the data still suggest that the amount of nanoplastics will be unexpectedly high. While these observations suggest that nanoplastics may be present in unexpectedly high amounts, it is not yet scientifically established whether nanoplastics accumulate in the environment, and if they do, the underlying mechanisms remain unclear.

<sup>a</sup> Biochemistry and Structural Biology, Lund University, Lund, Sweden.

E-mail: tommy.cedervall@chem.lu.se

<sup>b</sup> Nanolund, Lund University, Lund, Sweden

<sup>c</sup> Department of Applied Mechanics and Biomedical Engineering, Indian Institute of Technology Madras, Chennai-600036, India

<sup>d</sup> Department of Chemical Engineering, Indian Institute of Technology Madras, Chennai-600036, India



During the process of plastic degradation, it is anticipated that along with the release of small, dissolved molecules, the material breaks down progressively into smaller particles.<sup>9,10</sup> The combined breakdown effect of UV irradiation and mechanical degradation to form smaller particles and undetectable smaller substances has been shown on polypropylene, polyethylene and expanded polystyrene.<sup>11</sup> The aging of nanoplastics and its effect on physical parameters, environmental fate and changes in toxicity is well reviewed by Permana *et al.* in 2025.<sup>12</sup>

The degradation process of small nanosized particles is not yet understood. As the UVB irradiation can penetrate about 1–3  $\mu\text{m}$  into polystyrene,<sup>13,14</sup> it may not be feasible to think about a degradation process on the surface but rather a process that takes place on the entire particle. Furthermore, it can be anticipated that a large portion of the UVB radiation will pass through the particles without causing any damage. It was previously shown that high intensity UV irradiation on 0.2 to 5  $\mu\text{m}$  polystyrene particles resulted in a mass loss, prior to a decrease in the diameter,<sup>15</sup> strongly suggesting that the UV-mediated degradation did not only take place on the surface. Furthermore, we have previously noted that UVB treatment of amine-modified 54 nm polystyrene nanoparticles resulted in particles that had an apparent larger size when analysed with differential centrifugation sedimentation (DCS).<sup>16</sup> In contrast, the hydrodynamic size, as analysed by DLS (dynamic light scattering), was unchanged. Again, a possible explanation is that the UVB irradiation affects the entire particle and thereby decreases the mass, but the hydrodynamic size of the particle remains the same until the particle breaks down. There are studies partly contradicting these conclusions, as they show that the chemical changes occur mainly on the surface of the nanoplastics.<sup>17–19</sup>

Iron oxide, especially hematite, nanoparticles have been used in environmental remediation and in water treatment plants to remove various organic and inorganic substances.<sup>20</sup> One mechanism is the photoinduced production of reactive oxidative species on the surface of the nanoparticles, which will, in turn, react with the pollutant.<sup>20</sup> Hematite nanoparticles have been shown to increase the rate of the UV-mediated breakdown of microplastics.<sup>21</sup> If iron oxide can facilitate the breakdown of nanoplastics in the environment and water treatment plants, it could be a cheap and proven way to remove nanoplastics as it has already been tested successfully for other pollutants.

Although it may seem intuitive that UVC- and UVB-mediated degradation of nanoplastics increases with decreasing particle size, due to higher surface area at equal mass concentration, this relationship does not necessarily follow such straightforward scaling. The UV radiation can penetrate 1–3  $\mu\text{m}$  into polystyrene.<sup>14</sup> Therefore, if degradation occurs in the whole particle, larger particles can catch more of the light, whereas, progressively, more light can pass through small particles. Light will also scatter on larger particles and could then hit and react with another large particle. A dispersion with small particles will have more particles per

mass unit, while larger particles scatter more light. To better understand how nanoplastics of different sizes degrade, dispersion with the same mass needs to be tested.

## Results and discussion

### DCS as a method to assess the UVC-mediated PS breakdown

First, we wanted to test the hypothesis that UV irradiation affects the entire nanoparticle and that the process can thereby be followed using DCS (differential centrifugal sedimentation), as the sucrose will exchange with water, resulting in a particle with increased density and thereby an increased apparent size when analysed by DCS. Carboxylated polystyrene nanoparticles with a radius of 200 nm were irradiated with UVC for 24 hours. We chose UVC to shorten the experimental time. Particle samples were removed at the indicated times and analysed for size by DLS and DCS, as shown in Fig. 1a and b. The size changed quickly and progressively to larger sizes in DCS during the irradiation time, whereas the hydrodynamic size measured using DLS was the same. The hydrodynamic size will not be affected by the internal breakdown of the particle, whereas after UVC irradiation, the sucrose can occupy an increased volume within the particles. The polystyrene nanoparticles are in water and will encounter sucrose first after injection into the gradient. Therefore, we next investigated the effect of preincubating pristine polystyrene particles in sucrose before injecting them into the gradient. Fig. 1c shows a small increase in the apparent size after preincubation, indicating that sucrose can penetrate a limited volume of particles, most likely in the outer areas. The same experiment, using iron oxide particles, which are expected to be solid, showed no effect on the size after preincubation in sucrose, as shown in Fig. 1d. We thus conclude that DCS is a proficient method for scanning UV irradiation effects in nanoplastics prior to changes in hydrodynamic radius.

### UVB breakdown of different-sized polystyrene nanoparticles

Next, we investigated how particle size influences the breakdown of plain 99 and 195 nm polystyrene nanoparticles exposed to UVB irradiation. Fig. 2a shows that after 49 days of irradiation, the apparent size of the 195 nm nanoparticles starts to change, indicating that the breakdown process has taken place and progressed sufficiently to be detected by DCS. The breakdown process continues until the experiment is terminated after 107 days of irradiation. Fig. S1 shows the normalized data from day 7 and day 107, which highlights the shift in the apparent size. As expected, the size of the 195 nm nanoparticles in the control is much less affected. However, a fraction of the particles has a larger apparent size. This is probably due to the fact that some UVB irradiation leaks through the glass, as previously observed.<sup>16</sup> In contrast to the 195 nm nanoparticles, the size of the 99 nm particles appears to be less affected by UVB irradiation, as shown in Fig. 3a, with only a small change detected in the size, which is magnified in Fig. 3b. The breakdown process appears to have progressed over the 107 days; however, the rate of



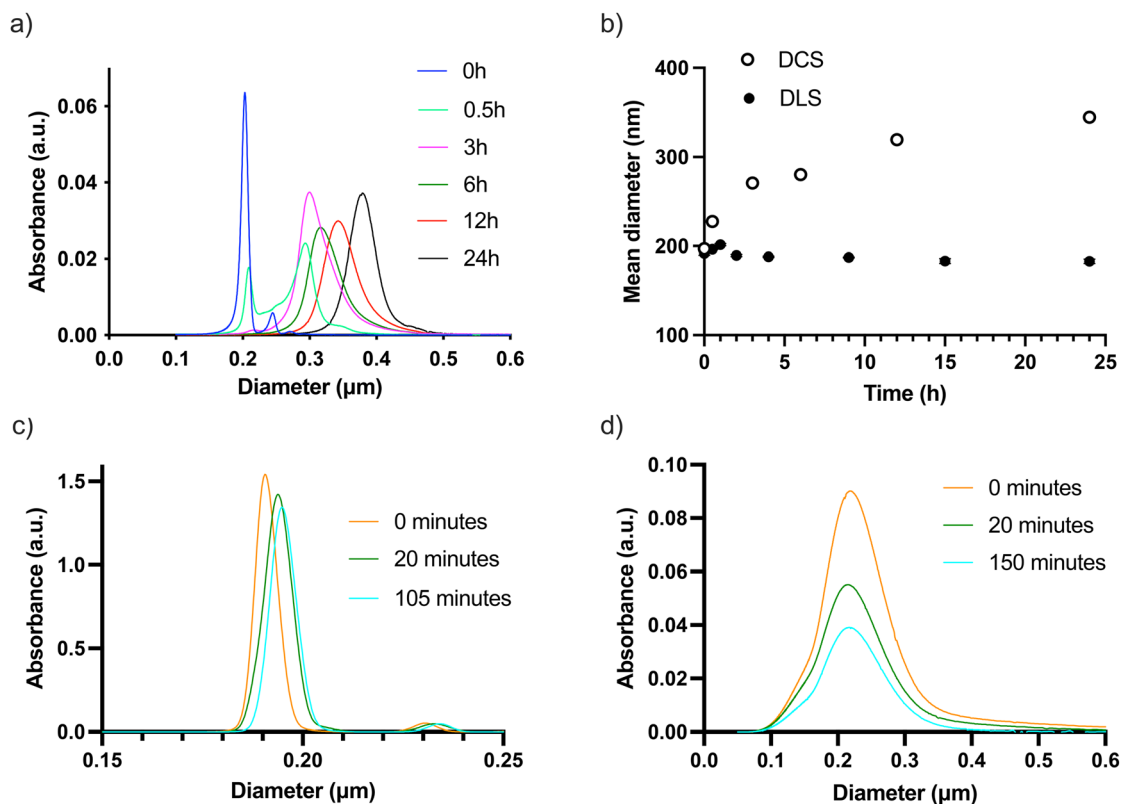


**Fig. 1** a. Size distribution measured using a disc centrifuge of 200 nm carboxylated polystyrene exposed to UVC for 24 h. b. Comparison of the average diameter of the 200 nm carboxylated polystyrene exposed to UVC for 24 h measured using DCS and DLS. c. Size distribution of polystyrene pre-incubated in sucrose corresponding to the initial sucrose concentration of the gradient. d. Size distribution of iron oxide in sucrose.

breakdown is much slower compared to the 195 nm particles. The mass of the 195 and 99 nm nanoparticles was the same in the two experiments; thus, the number of particles was about 8 times higher in the 99 nm nanoparticles.

#### UVB-mediated breakdown in the presence of iron oxide nanoparticles

Next, we investigated whether the presence of iron oxide particles will affect the UVB-mediated breakdown. The

rationale is, as described above, that UVB irradiation of the iron oxide surface generates reactive oxidative species, which will speed up the breakdown of polystyrene. In the mixture of iron oxide,  $\text{Fe}_2\text{O}_3$ , and 195 nm polystyrene nanoparticles, strong visible aggregation was observed, which made further analysis impossible. The iron oxide nanoparticles have a pH-dependent surface charge and at neutral pH, iron oxide particles have a small positive Z-potential. Polystyrene has negatively charged sulfone groups, and the aggregation is likely driven by electrostatic

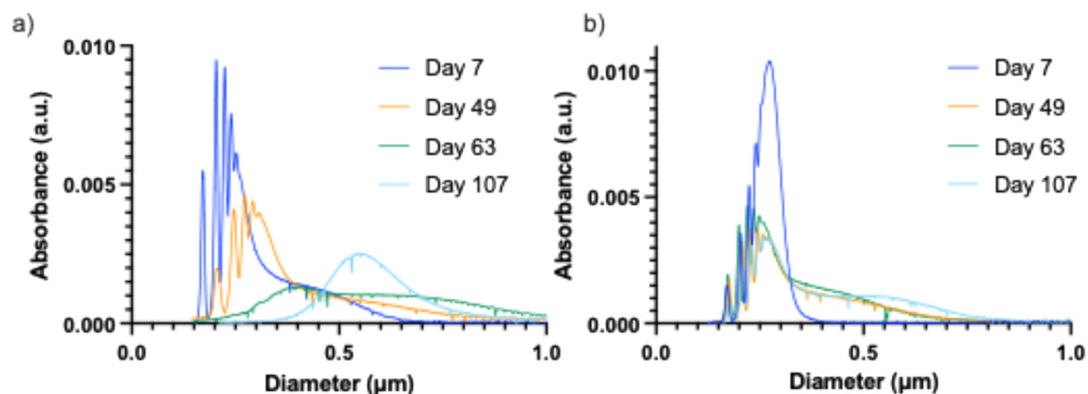


**Fig. 2** DCS analyses of 195 nm polystyrene nanoparticles: a. UVB-treated nanoparticles and b. Non UVB-treated nanoparticles.



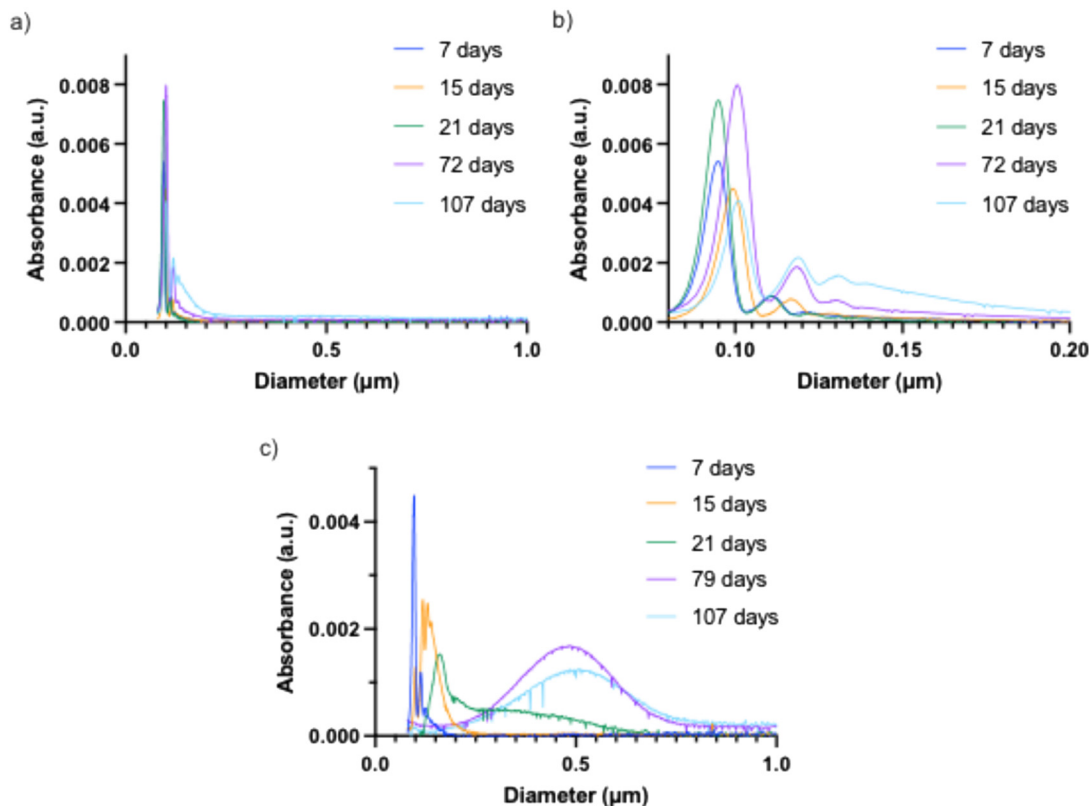


Fig. 3 DCS analyses of 99 nm polystyrene nanoparticles: a. UVB-treated nanoparticles, b. magnified UVB-treated nanoparticles, and c: UVB-treated nanoparticles, together with iron oxide nanoparticles.

attractions. However, no aggregation was observed when added together with the 99 nm polystyrene nanoparticles. Instead, we observed changes in the apparent size already after 15 days of UVB irradiation, as shown in Fig. 3c. The breakdown seemed to continue until the experiment was terminated after 107 days.

Although the raw DCS data indicate differences in how fast the breakdown occurs, we wanted to be able to compare the different breakdown situations in a time-resolved way. It is challenging to quantitatively compare data from different days due to differences in the sucrose gradient and loading volumes. This was overcome by calculating different ratios for each experimental day. Thereafter, data from the different days could be compared. First, the largest average size from the control was divided by the average size from each run; thus, as the fraction of apparently larger particles increases, the ratio decreases. Next, we recalculated the DCS data to estimate the amount of material, assuming that the particles, regardless of size, were spherical. Thereafter, we calculated the mass ratio between nanoparticles with a size below 250 nm and the total mass; thus, if the apparent size increased because of UVB-mediated breakdown, the ratio decreased. The results are shown in Fig. 4a and b. Only small changes can be observed for the 99 nm polystyrene nanoparticles, but for the 195 nm polystyrene nanoparticles and for the mixture of 99 nm polystyrene and iron oxide nanoparticles, a clear change can be seen. Comparing the two breakdowns also

clearly shows that the breakdown occurs much faster when iron oxide nanoparticles are present.

Simultaneously with DCS measurements, the size of the nanoparticles was also determined by DLS, as shown in Fig. 4c. The controls and the UVB-irradiated 99 nm polystyrene nanoparticle samples showed no change in size. In the 195 nm polystyrene and the mixture containing iron oxide and 99 nm polystyrene nanoparticles, it was not possible to follow the size decrease throughout the experiment due to low intensity in the DLS signal. However, interestingly, we could see that the size of the 195 nm was smaller compared to the control shortly after the UVB irradiation, as shown in Fig. 4c, possibly due to chemical changes in the surface decreasing the tendency for aggregation. In the mixture containing iron oxide and 99 nm polystyrene nanoparticle, an increased size was observed after two weeks of UVB irradiation, as displayed in Fig. 4c. However, the decreasing quality of the size data over time (Table S1), likely caused by very low signal intensity, suggests that the observed aggregation may be an artifact arising from the detection limits of the instrument.

Examining the DLS data, we noticed that with time, the reported intensity decreased in the 195 nm polystyrene nanoparticles, and in the mixture of iron oxide and 99 nm polystyrene nanoparticles. This made a time resolved size evaluation impossible. However, the DLS software was set on a self-attenuation mode. This means that the laser power and detector sensitivity is automatically set to achieve the best



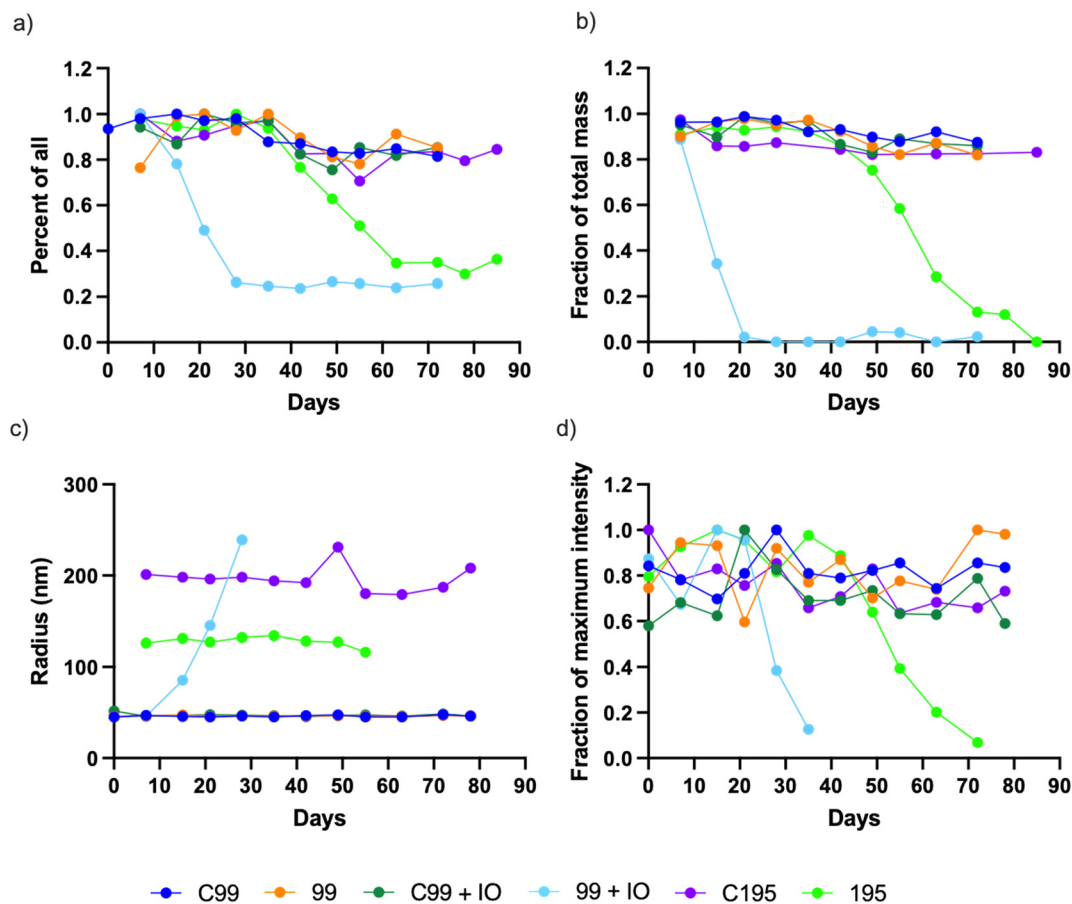


**Fig. 4** a. Ratio between the average of large and small sizes calculated from DCS. C99: non UVB-irradiated nanoparticles, 99: UVB-irradiated nanoparticles, C99 + IO: non UVB-irradiated nanoparticles together with iron oxide nanoparticles, 99 + IO: UVB-irradiated nanoparticles, together with iron oxide nanoparticles, C195: non UVB-irradiated 195 nm nanoparticles, and 195: UVB-irradiated 195 nm nanoparticles. b. Percentage of total mass within the range of the starting material as calculated from DCS. c. DLS size plot. d. Fraction of weekly DLS intensity divided with maximum DLS intensity over the whole experiment. The DLS data and statistics for some time points are presented in Table S1.

possible total intensity, which is normally around  $10^8$  counts per second. With decreasing particle concentration, this is eventually not achievable, and the intensity decreases. Thus, a decreased intensity could be carefully interpreted as a decrease in particle concentration, a change in the refractive index, and/or a reduction in density compared to the original particles. To explore this possibility, we divided the intensity measured from each week by the largest intensity measured at all weeks. The result in Fig. 4d shows that although the variation between the different time points is large, the intensity from 195 nm polystyrene, and the 99 nm + IO nanoparticles seem to disappear at the same time as the sizes increase in the DCS experiments.

After 111 days of UVB exposure, the experiment was terminated and all samples were centrifuged. A pellet was observed only in the 99 + IO sample. The size of the remaining nanoparticles was determined by DLS and NTA, and the concentrations were estimated by NTA (Table 1). There are about 100 times fewer particles in the 99 + IO and in the resulting pellet compared to the control sample and the 99 nm sample, confirming that the particles are broken

down to a great extent in the 99 + IO sample. Interestingly, the remaining particles appear to have the same size as in the control. The concentration of the 195 nm particles could not be reliably measured due to growth in the sample, but measurements indicated a lower concentration compared to the control.

### Size-dependent mechanical breakdown of polystyrene nanoparticles

Next, we investigated whether the mechanical breakdown of polystyrene nanoparticles is size-dependent. If both mechanical and UVB-mediated degradation exhibit size dependence, these processes may contribute to an accumulation of plastics in the nanoscale range. We have previously investigated the breaking down of a variety of plastics to nanoparticles using mechanical forces from a blender.<sup>22,23</sup> The size of the formed particles is between 100 and 200 nm, and, interestingly, we were not able to detect smaller nanoparticles, indicating that there is a size limitation. We subjected the 2  $\mu\text{m}$  and 99 nm particles for this treatment for 25 min. Characterization of the 2  $\mu\text{m}$



**Table 1** Concentration and size of the nanoparticles after 111 days of UV treatment

Particle	Concentration <sup>a</sup> (particles per mL)	NTA diameter <sup>b</sup> (nm)	DLS diameter (nm)	DLS PD <sup>c</sup> (%)
99	$3.0 \times 10^{11} \pm 1.1 \times 10^{10}$	$86.6 \pm 0.6$	$88.0 \pm 1.7$	$9.5 \pm 2.5$
C99	$2.0 \times 10^{11} \pm 6.3 \times 10^9$	$96.8 \pm 1.4$	$87.5 \pm 0.7$	$6.3 \pm 1.8$
99 + IO	$6.1 \times 10^8 \pm 0.8 \times 10^7$	$140 \pm 5$	ND	ND <sup>d</sup>
C99 + IO	$1.9 \times 10^{11} \pm 1.2 \times 10^{10}$	$91.1 \pm 0.2$	ND	ND
P99 + IO <sup>e</sup>	ND	ND	ND	ND

<sup>a</sup> Measured by NTA. <sup>b</sup> Mean diameter. <sup>c</sup> Polydispersity. <sup>d</sup> Concentration too low for reliable data. <sup>e</sup> Pellets from the 99 + IO sample dispersed in the same volume as before centrifugation.

nanoparticles over time using DCS showed that the size of the nanoparticles remained the same, except for the growth of a larger fraction, Table S2. However, the amount of material decreased (Fig. 5 and Table S2). If smaller particles are produced during the mechanical breakdown, they may not be detectable by DCS, especially if the 2  $\mu\text{m}$  particles are still dominating. Therefore, we filtered all samples through a filter with at a 0.8  $\mu\text{m}$  cut off. However, after filtration, we could not detect any particles using DCS. Small particles, however, can be detected with NTA and DLS. Analyses of the untreated 2  $\mu\text{m}$

polystyrene particles using NTA shows that there is a fraction of smaller particles with a diameter around 290 nm (Table S3). However, with the mechanical breakdown, there are smaller particles appearing probably due to breakdown of the larger particles (Table S3). Furthermore, the particle concentration increases with time (Fig. 5b, Table S3). The quality of the DLS measurement was too low. However, after filtering the breakdown samples with 0.8  $\mu\text{m}$  filters, it was possible to detect a particle size of about 65 nm (Table S4). The quality of the DLS data was still low and each of the 30 acquisitions was evaluated and only those with good quality were used (Table S4). The decrease of mass measured with DCS together with the increase in concentration of smaller particles measured by NTA strongly suggest that the 2  $\mu\text{m}$  polystyrene particles are broken down by mechanical treatment. The 99 nm particles are much less affected as the size measured by DCS and DLS is the same after breakdown and only a small decrease in the total mass and an increase in particle concentration can be detected at the end of the breakdown (Fig. 5, Tables S1–S3). Furthermore, the size of small particles produced from the breakdown of the 2  $\mu\text{m}$  particles remain the same over the breakdown period (Tables S3 and S4). Taken together, the data show that larger particles are mechanically broken down to smaller particles, whereas smaller particles are not, suggesting that there is a size limit for an effective breakdown in our system. We do not have a definitive explanation for this observation; however, we speculate that the microfluidic environment may confer protection to smaller particles.

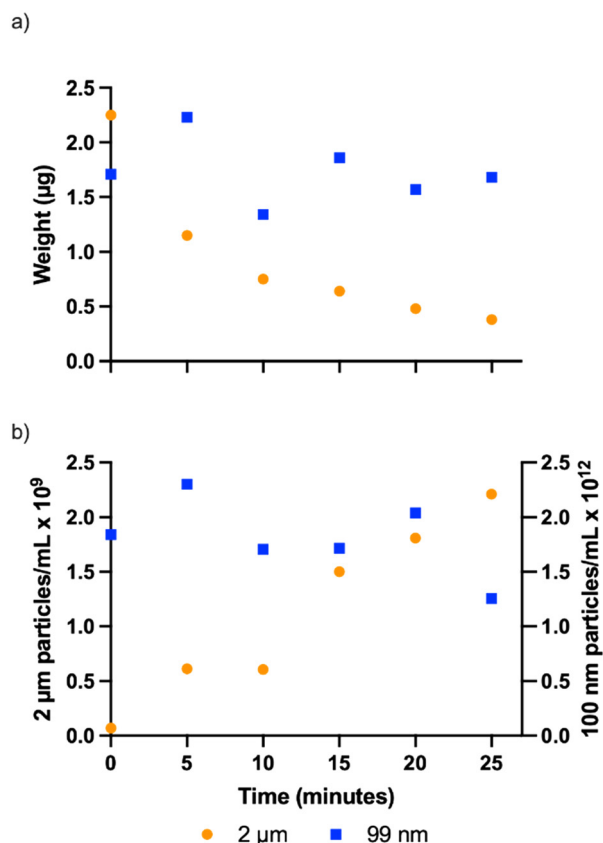


**Fig. 5** Characteristics of the 2  $\mu\text{m}$  and 99 nm polystyrene nanoparticles after mechanical breakdown. a. Estimated total weight calculated from DCS data for peaks around 100 and 1700 nm. b. Particle concentration of the small particles resulting from the mechanical breakdown of 2  $\mu\text{m}$  polystyrene particles and the 99 nm particles estimated from NTA data. The data is from samples filtered through a 0.8  $\mu\text{m}$  filter. The size of the 2  $\mu\text{m}$  particles decreases with time (see Table S3).

#### Toxicity of UVB breakdown products on *Daphnia magna*

Next, we investigated the effect of UVB irradiation on the 99 nm polystyrene nanoparticles, with or without iron oxide nanoparticles, on toxicity to *D. magna*. A Kaplan–Meier survival analysis showed that combining the 99 nm polystyrene nanoparticles with iron oxide nanoparticles and UVB exposure removed the toxicity of the supernatant as compared to the control ( $p > 0.05$ , Fig. 6 and Table 2). All other treatments with the 99 nm polystyrene particle showed toxicity compared to both the control and the UVB-exposed 99 nm treatment with iron oxide ( $p$  is always  $< 0.001$ , Fig. 6 and Table 2). No significant differences in toxicity were observed among the other 99 nm-treated samples, which were not exposed to both UVB and iron oxide ( $p > 0.05$ , Fig. 6 and Table 2). The concentration of the 99 nm plain



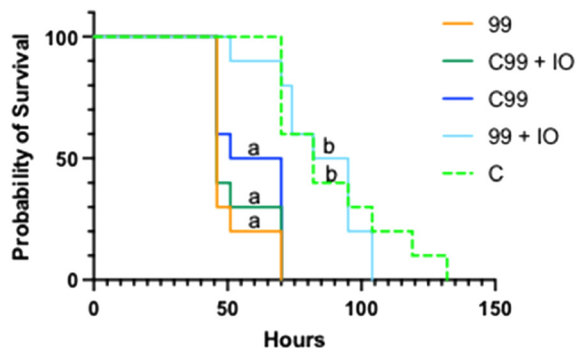


**Fig. 6** Kaplan–Meier survival analysis of the supernatant after the UVB breakdown of 99 nm polystyrene nanoparticles in the presence or absence of iron oxide particles (IO). 99 denotes UVB-exposed particles, C99 denotes UV-shaded particles, and C denotes a control treatment with only artificial freshwater.

**Table 2** Statistical cross comparisons of survival data

Compared treatments	Log-rank (Mantel–Cox) test			Significance
	$\chi^2$	d.f.	<i>p</i>	
Global ( <i>all treatments</i> )	34.22	4	<0.0001	****
C–C 99 MQ	11.06	1	0.0009	***
C–99 MQ + UV	15.18	1	<0.0001	****
C–C 99 IO	13.47	1	0.0002	***
C–99 IO + UV	0.3486	1	0.5549	n.s.
C 99 MQ–99 MQ + UV	1.987	1	0.1587	n.s.
C 99 MQ–C 99 IO	0.8264	1	0.3633	n.s.
C 99 MQ–99 IO + UV	12.26	1	0.0005	***
99 MQ + UV–C 99 IO	0.2574	1	0.6119	n.s.
99 MQ + UV–99 IO + UV	16.05	1	<0.0001	****
C 99 IO–99 IO + UV	14.53	1	0.0001	***

d.f. denotes degrees of freedom, *p* denotes *p*-value, asterisks highlight statistically significant differences, and n.s. denotes not significant.

polystyrene nanoparticles is approximately 50 mg L<sup>-1</sup>, and toxicity has been observed at similar concentrations. After the UVB irradiation of 99 + IO, the concentration is very low (Table 1). Therefore, the loss of toxicity of the 99 + IO sample is likely due to a decreased particle concentration.

### Overall discussion

Our data suggest that the effect of UVB irradiation and mechanical force on the breakdown of polystyrene nanoparticles is much slower on smaller nanoparticles, 99 nm, than on larger particles, 195 nm (UVB) and 2 μm (mechanical). In experiments using high intensity UV irradiation on different-sized polystyrene particles, there was no difference in the breakdown rate.<sup>15</sup> Furthermore, it was shown that there was a loss of mass, before a size decrease was observed. In these experiments a complete breakdown was seen by measuring the total carbon (TOC). If a size-dependent breakdown of plastics is true for naturally occurring micro- and nano-plastics in nature, it would lead to an accumulation of small-sized nanoplastics. Nanoplastics are difficult to detect in nature but recent data on the size

distribution of micro- and nano-plastics suggest that the amount of nanoplastics is surprisingly high.<sup>2,7</sup> Our data could be part of an explanation of an unexpected high concentration of nanoplastics.

We could detect only a minor breakdown of the 99 nm polystyrene nanoparticles after 110 days of UVB irradiation. However, the addition of iron oxide nanoparticles to the reaction increased the breakdown rate significantly. This effect of iron oxide has been shown for larger microplastics.<sup>21</sup> This is promising as it suggests that iron oxide could be used as a remediation substance in nature for nanoplastics and in water treatment plants, despite the size-dependent UVB-mediated breakdown. Furthermore, the strong effect of iron oxide implies that the plastic breakdown could be very different at different locations in nature depending on the presence of naturally occurring iron oxides.

We have previously reported that the UVB-mediated breakdown of amine-modified polystyrene nanoparticles decreased the toxicity of the particles themselves,<sup>16</sup> whereas the small, dissolved molecules from the breakdown exhibited toxicity. Here, we do not observe an effect on toxicity before the particles are mainly broken down in the presence of iron oxide. The decreased toxicity after breakdown indicates that the breakdown process does not result in toxic small, dissolved molecules. However, as the experiments lasted for 111 days, volatile, possibly toxic, substances are not present. Overall, there is limited knowledge on how UVB irradiation and breakdown of nanoplastics influence the toxicity.<sup>12</sup>

## Materials and methods

### Polystyrene and iron oxide nanoparticles

The polystyrene nanoparticles were from Bangs Inc, USA. The specific batches used were for carboxylated 200 nm, inv# L110506B, unmodified 99 nm; Inv# L100215B Lot# 9598, and unmodified 195 nm; Inv# L190509D Lot# 14286. Before use, the particles were diluted ten times and extensively dialysed against MilliQ water to remove the additives, NaN<sub>3</sub> and Tween20, and the remaining dissolved polymers. Iron oxide, Fe<sub>2</sub>O<sub>3</sub>, was from Nanoshell UK Ltd, Great Britain, batch number NS6130-03-318. Before use, the iron oxide particles were sonicated in an ultrasound bath (Elmasonic P, Elma Schmidbauer GmbH, Singen, Germany) filled with water at 100% power, 37 kHz, 22 °C for 60 × 3 min. In between the 60 minute runs, the ultrasound bath was cooled for approximately 10 minutes.

### UVC irradiation

The particles were diluted 10× with MilliQ water, transferred to a dialyzing tube (MilliPore MWCO 3000) and dialyzed against MilliQ water. The dialyzed particles were diluted 76× with MilliQ water to a final concentration of ≈0.013% (W/W) or ≈0.13 mg dm<sup>-3</sup>. 380 mL of the dialyzed particle solution was transferred to a 600 mL glass beaker. The UV-C lamp was submerged in the solution such that the end of the lamp was 2–5 mm above the bottom of the glass beaker. Two glass



tubes connected *via* a peristaltic pump were also submerged in the glass beaker (see Fig. S3). The setup was placed in a room that was held at 4–8 °C, and the particle solution was constantly pumped during the UV-C treatment. The UV-C treatment was for 24 h and samples were taken at specified time points. The particle solution had a temperature of 20–22 °C for over 24 hours. The UVC lamp emission spectrum is shown in Fig. S4.

### UVB irradiation

The particles were diluted another 200 times in MilliQ water or in iron oxide to an estimated final polystyrene concentration of 100  $\mu\text{g mL}^{-1}$ . For the UVB irradiation, 70 mL of each particle was placed in glass petri dishes with a quartz top for the test sample and with a glass top for the control and subjected to UVB. UV-B lamps (ExoTerra Reptile UV-B 200, 25 W) were purchased from a local pet shop. The UVB irradiation and the emitted wavelength spectra have been reported.<sup>16</sup> The UVB dose is 225  $\mu\text{W cm}^{-2}$  and 10 cm from the lamp. The volume was adjusted regularly to compensate for evaporation. Samples were taken out at the indicated times during the 111-day irradiation period and analysed for size by DCS, DLS and for size and concentration by NTA.

### Mechanical breakdown

Polystyrene with a diameter of 2  $\mu\text{m}$  or 100 nm was broken down as described previously for larger plastics.<sup>22,23</sup> The breakdown was done in water and continued for 25 minutes. Every 5th minute, the samples were taken out and analysed for size by DCS and DLS.

### Differential centrifugal sedimentation

The samples were analysed as indicated on a DC24000 disc centrifuge (CPS Instruments, USA). The sucrose gradient used for polystyrene was 4–12% in water and the centrifugal speed was 24 000 RPM, while for iron oxide samples it was 8–24% and the speed 1842 RPM. The temperature was approximately 23 °C. The sample volume was 100  $\mu\text{L}$ . The detector wavelength is 405 nm. Before each new sample, the gradient was calibrated using 0.545 nm PVC (polyvinyl chloride) particles. All samples were analyzed using an identical gradient setup, and calibration between runs was performed to minimize the impact of gradient variability. Normally, the samples were applied to the sucrose gradient without the preincubation in sucrose. In the experiments in which preincubation is indicated, the samples were mixed with sucrose so that the final concentration of sucrose equals that of the sucrose concentration at the beginning of the sucrose gradient, *i.e.*, 4% for polystyrene and 8% for iron oxide. The instrument was controlled and the data was analysed with the DCCS (Disc Centrifuge Control System) program v.11 (CPS Instruments, USA). The particles were assumed to be spherical for all calculations.

### Dynamic light scattering

The samples were analysed as indicated for DLS using a DynaPro Plate Reader II from Wyatt Technology, USA. The laser strength and the detector sensitivity were set by the auto attenuation function. The temperature was 23 °C, and 20 acquisitions were obtained for each sample with a 10 second acquisition time. The laser wavelength was 821.5 nm.

### Toxicity studies and statistical analyses

At the end of the UVB irradiation period, the acute toxicity was tested on zooplankton *Daphnia magna* (*D. magna*). The toxicity tests were performed in 10 replicates with a total volume of 9 mL in each test tube. Each sample consisted of 4.5 mL of collected fractions mixed with 4.5 mL of double concentrated ISO test water. For the controls, 4.5 mL of Milli-Q water was mixed with 4.5 mL of double concentrated ISO test water. The ISO test water used was prepared according to the OECD 202 test guidelines.<sup>24</sup> The particle concentration was approximately 50  $\text{mg L}^{-1}$ . The survival was checked regularly for 24 hours. The *D. magna* survival in acute toxicity tests was evaluated using Kaplan–Meier survival analysis and the *p*-value was attained from the log-rank (Mantel–Cox) test. All statistical evaluations were performed using GraphPad Prism (version 8.4.3).

## Conclusions

-UVB irradiation affects larger polystyrene nanoparticles faster than smaller particles.

-Mechanical force affects larger polystyrene nanoparticles more than smaller particles.

-Iron oxide nanoparticles speed up the effect of UVB irradiation.

-Small, dissolved molecules from the breakdown are not toxic to *D. magna*.

## Author contributions

MTE – conceptualization, investigation, and writing – review and editing. RS – investigation and writing – review and editing. SS – conceptualization and writing – review and editing. EM – conceptualization and writing – review and editing. ML – conceptualization, investigation, and writing – review and editing. TC – conceptualization, investigation, writing – original draft, and writing – review and editing.

## Conflicts of interest

There are no conflicts to declare.

## Data availability

The data supporting this article have been included as part of the SI.

Supplementary information (SI) is available. See DOI: <https://doi.org/10.1039/d5en00848d>.



## Acknowledgements

T. C. acknowledge financial support from the Swedish research council FORMAS through grant nr.: 2022-02284 and 2022-01128. M. T. E. acknowledge financial support from the Swedish research council FORMAS through grant nr.: 2023-00504.

## References

- 1 A. Ter Halle, L. Jeanneau, M. Martignac, E. Jardé, B. Pedrono and L. Brach, *et al.*, Nanoplastic in the North Atlantic Subtropical Gyre, *Environ. Sci. Technol.*, 2017, **51**(23), 13689–13697.
- 2 S. ten Hietbrink, D. Materić, R. Holzinger, S. Groeskamp and H. Niemann, Nanoplastic concentrations across the North Atlantic, *Nature*, 2025, **643**(8071), 412–416.
- 3 D. Materić, E. Ludewig, D. Brunner, T. Röckmann and R. Holzinger, Nanoplastics transport to the remote, high-altitude Alps, *Environ. Pollut.*, 2021, **288**, 117697.
- 4 D. Materić, H. A. Kjær, P. Vallelonga, J. L. Tison, T. Röckmann and R. Holzinger, Nanoplastics measurements in Northern and Southern polar ice, *Environ. Res.*, 2022, **208**, 112741.
- 5 D. Materic, M. Peacock, J. Dean, M. Futter, T. Maximov and F. Moldan, *et al.*, Presence of nanoplastics in rural and remote surface waters, *Environ. Res. Lett.*, 2022, **17**(5), 054036.
- 6 D. Materic, R. Holzinger and H. Niemann, Nanoplastics and ultrafine microplastic in the Dutch Wadden Sea – The hidden plastics debris?, *Sci. Total Environ.*, 2022, **846**, 157371.
- 7 S. Fraissinet, G. E. De Benedetto, C. Malitesta, R. Holzinger and D. Materić, Microplastics and nanoplastics size distribution in farmed mussel tissues, *Commun. Earth Environ.*, 2024, **5**(1), 128.
- 8 N. Yakovenko, L. Pérez-Serrano, T. Segur, O. Hagelskjaer, H. Margenat and G. Le Roux, *et al.*, Human exposure to PM10 microplastics in indoor air, *PLoS One*, 2025, **20**(7), e0328011.
- 9 B. Gewert, M. Plassmann and M. MacLeod, Pathways for degradation of plastic polymers floating in the marine environment, *Environ. Sci.: Processes Impacts*, 2015, **17**(9), 1513–1521.
- 10 K. Zhang, A. Hamidian, A. Tubic, Y. Zhang, J. Fang and C. Wu, *et al.*, Understanding plastic degradation and microplastic formation in the environment: A review, *Environ. Pollut.*, 2021, **274**, 116554.
- 11 Y. Song, S. Hong, M. Jang, G. Han, S. Jung and W. Shim, Combined Effects of UV Exposure Duration and Mechanical Abrasion on Microplastic Fragmentation by Polymer Type, *Environ. Sci. Technol.*, 2017, **51**(8), 4368–4376.
- 12 R. Permana, S. Chakraborty and E. Valsami-Jones, Nanoplastics in aquatic environments: The hidden impact of aging on fate and toxicity, *Environ. Chem. Ecotoxicol.*, 2025, **7**, 429–444.
- 13 Z. Kanuchová, G. Baratta, M. Garozzo and G. Strazzulla, Space weathering of asteroidal surfaces Influence on the UV-Vis spectra, *Astron. Astrophys.*, 2010, **517**(A60), DOI: [10.1051/0004-6361/201014061](https://doi.org/10.1051/0004-6361/201014061).
- 14 K. Monsores, A. da Silva, S. Oliveira, R. Weber, P. Feliciano and S. Monteiro, Influence of ultraviolet radiation on polystyrene, *J. Mater. Res. Technol.*, 2021, **13**, 359–365.
- 15 G. Balakrishnan, F. Lagarde, C. Chassenieux, A. Martel, E. Deniau and T. Nicolai, Fate of polystyrene and polyethylene nanoplastics exposed to UV in water, *Environ. Sci.: Nano*, 2023, **10**(9), 2448–2458.
- 16 M. T. Ekvall, R. Svensson, J. García Martínez, A. M. Kraiss, K. Bernfur and T. Leiding, *et al.*, UV-B degradation affects nanoplastic toxicity and leads to release of small toxic substances, *Environ. Sci.: Nano*, 2025, **12**(2), 1177–1185.
- 17 Z. Liu, Y. Zhu, S. Lv, Y. Shi, S. Dong and D. Yan, *et al.*, Quantifying the Dynamics of Polystyrene Microplastics UV-Aging Process, *Environ. Sci. Technol. Lett.*, 2022, **9**(1), 50–56.
- 18 S. Peng, L. Li, D. Wei, M. Chen, F. Wang and Y. Gui, *et al.*, Releasing characteristics of toxic chemicals from polystyrene microplastics in the aqueous environment during photoaging process, *Water Res.*, 2024, **258**, 121768.
- 19 L. Tian, Q. Chen, W. Jiang, L. Wang, H. Xie and N. Kalogerakis, *et al.*, A carbon-14 radiotracer-based study on the phototransformation of polystyrene nanoplastics in water versus in air, *Environ. Sci.: Nano*, 2019, **6**(9), 2907–2917.
- 20 D. Chaudhari, R. Upadhyay, G. Shinde, M. Gawande, J. Filip and R. Varma, *et al.*, A review on sustainable iron oxide nanoparticles: syntheses and applications in organic catalysis and environmental remediation, *Green Chem.*, 2024, **26**(13), 7579–7655.
- 21 L. Ding, X. Guo, S. Du, F. Cui, Y. Zhang and P. Liu, *et al.*, Insight into the Photodegradation of Microplastics Boosted by Iron (Hydr)oxides, *Environ. Sci. Technol.*, 2022, **56**(24), 17785–17794.
- 22 M. T. Ekvall, I. Gimskog, J. Hua, E. Kelpsiene, M. Lundqvist and T. Cedervall, Size fractionation of high-density polyethylene breakdown nanoplastics reveals different toxic response in *Daphnia magna*, *Sci. Rep.*, 2022, **12**(1), 3109.
- 23 M. T. Ekvall, M. Lundqvist, E. Kelpsiene, E. Šileikis, S. B. Gunnarsson and T. Cedervall, Nanoplastics formed during the mechanical breakdown of daily-use polystyrene products, *Nanoscale Adv.*, 2019, **1**(3), 1055–1061.
- 24 OECD Test No. 202: *Daphnia sp.* Acute Immobilisation Test, 2004.

